ESMO Open
Cancer Horizons

Check for updates

Four distinct immune microenvironment subtypes in gastric adenocarcinoma with special reference to microsatellite instability

Junhun Cho,[1] Young Hwan Chang,[2] You Jeong Heo,[3] Seungtae Kim,[3] Nayoung KD Kim,[4] Joon Oh Park,[3] Won Ki Kang,[3] Jeeyun Lee,[3] Kyoung-Mee Kim[1]

► Additional material is published online only. To view please visit the journal online (http://dx.doi.org/10.1136/esmoopen-2018-000326).

To cite: Cho J, Chang YH, Heo YJ, *et al*. Four distinct immune microenvironment subtypes in gastric adenocarcinoma with special reference to microsatellite instability. *ESMO Open* 2018;**3**:e000326. doi:10.1136/esmoopen-2018-000326

JC and YHC contributed equally.

Received 12 January 2018
Revised 6 February 2018
Accepted 15 February 2018

[1]Department of Pathology and Translational Genomics, Samsung Medical Center, Sungkyunkwan University School of Medicine, Seoul, Korea
[2]Department of Biomedical Engineering and Computational Biology Program, Oregon Health and Science University (OHSU), Portland, Oregon, USA
[3]Division of Hematology-Oncology, Department of Medicine, Samsung Medical Center, Sungkyunkwan University School of Medicine, Seoul, Korea
[4]Samsung Genome Institute, Samsung Medical Centre, Seoul, Korea

Correspondence to
Dr Kyoung-Mee Kim; kkmkys@skku.edu

ABSTRACT

Introduction Programmed death-ligand 1 (PD-L1) can be overexpressed in tumours other than Epstein-Barr virus (EBV)-positive (EBV$^+$) or microsatellite instability-high (MSI-H) gastric cancer (GC) subtypes. We aimed to determine the tumour immune microenvironment (TME) classification of GC to better understand tumour–immune interactions and help patient selection for future immunotherapy with special reference to MSI-H.

Methods Immunohistochemistry (IHC) for PD-L1 and CD8$^+$ T cells in three distinct subtypes of GC (43 EBV$^+$, 79 MSI-H and 125 EBV$^-$/MSS) were performed and analysed. In 66 MSI-H GC, mutation counts were compared with PD-L1 expression and survival of the patients.

Results GC TME divided by PD-L1 IHC and tumour-infiltrating lymphocytes (TIL) measured by intratumoural CD8 density showed: (1) about 40% of GC are type I (PD-L1$^+$/TIL$^+$) consisting ~70% of MSI-H or EBV$^+$ GC, and ~15% of EBV$^-$/microsatellite stable (MSS) GC patients show the best survival in both disease-free (HR 2.044) and overall survival (HR 1.993); this type would respond to a checkpoint blockade therapy; (2) almost 30% of GC are type II (PD-L1$^-$/TIL$^-$) with the worst survival; (3) approximately 10% of GC are type III (PD-L1$^+$/TIL$^-$); and (4) up to 20% are type IV (PD-L1$^-$/TIL$^+$) and, unexpectedly, ~25% of EBV$^+$ or MSI-H GC are within this subtype. In MSI-H GC, frequent frameshift mutations were observed in *ARID1A*, *RNF43*, *NF1*, *MSH6*, *BRD3*, *NCOA3*, *BCORL1*, *TNKS2* and *NPM1* and the numbers of frameshift mutation correlated significantly with PD-L1 expression ($P<0.05$).

Discussion GC can be classified into four TME types based on PD-L1 and TIL, and numbers of frameshift mutation correlate well with PD-L1 expression in MSI-H GC.

Key questions

What is already known about this subject?

- There is an urgent need to comprehensively understand tumour microenvironments (TME) and tumour-immune interactions in gastric cancer (GC).
- In GC, the frequency of programmed death-ligand 1 (PD-L1) expression approached 40%. However, not all Epstein-Barr virus (EBV)-positive (EBV$^+$) or microsatellite instability-high (MSI-H) GC overexpress PD-L1, and PD-L1 can be overexpressed in GC tumours other than EBV$^+$ or MSI-H GC.
- This warrants further TME classifications in association with the treatment strategies for immunotherapy.

What does this study add?

- We measured the expression of PD-L1 and CD8$^+$ T cell density in three distinct subtypes of GC (43 EBV$^+$, 79 MSI-H and 125 EBV$^-$/microsatellite stable) in relation to host antitumour immunity.
- We could divide four GC TME subtypes by PD-L1 expression and tumour-infiltrating lymphocytes (TIL) measured by intratumoural CD8 density. The frequencies and prognosis of four GC TME subtypes are similar to the previous study on melanoma patients.
- We compared the mutation loads with PD-L1 expression and survival in MSI-H GC patients. In MSI-H GC, the numbers of frameshift mutation correlated significantly with PD-L1 overexpression.

How might this impact on clinical practice?

- GC can be classified into four TME types based on PD-L1 and TIL and numbers of frameshift mutation correlate well with PD-L1 expression in MSI-H GC.

INTRODUCTION

Gastric cancer (GC) is a common disease with limited treatment options and poor prognosis.[1 2] Recently, great progress in cancer immunotherapy has created a new era of cancer treatment.[3] Among the most promising approaches for activating therapeutic anti-tumour immunity, blockade of the immune checkpoints programmed cell death protein 1 (PD-1) and cytotoxic T-lymphocyte-associated protein 4 has been most successful.[4] Given the immunomodulatory mechanism-of-action of immunotherapy and dynamic interactions between tumour cells and tumour microenvironments (TME), there is an urgent need to comprehensively understand tumourimmune interactions in GC.[5]

Programmed death-ligand 1 (PD-L1) is a PD-1 ligand that is overexpressed in many malignancies. PD-L1 can inhibit cytokine production and the cytolytic activity of PD-1$^+$ tumour-infiltrating CD4$^+$ and CD8$^+$ T cells.[6–8] These properties make PD-L1 a promising target for cancer immunotherapy. Recently, the classification of tumours into four TME types based on their PD-L1 status and the presence or absence of tumour-infiltrating lymphocytes (TILs) has been proposed and validated in melanoma.[6 9] These TME subtypes include type I (PD-L1$^+$/TIL$^+$ driving adaptive immune resistance; 38%), type II (PD-L1$^-$/TIL$^-$ indicating immune ignorance; 41%), type III (PD-L1$^+$/TIL$^-$ indicating intrinsic induction of PD-L1 by oncogenic pathway; 1%) and type IV (PD-L1$^-$/TIL$^+$ indicating the role of other suppressors in promoting immune tolerance; 20%).[10] Type I cancers may be most likely to respond to PD-1/PD-L1 blockade, and the proportion of various human tumours that fit into each of these TME types likely depends on genetic aberrations and oncogene drivers of the cancer as well as the tissue in which they arise.[9]

Given that immune infiltrates are heterogeneous between tumour types and are highly diverse between patients,[11] exploring the in silico immune contexture is critical for tailoring successful immunotherapy. In GC, PD-L1/TIL status generated by similar methodologies has been recently reported; however, the results are limited by (A) the relatively small number of cases (n=34),[12] (B) tissue microarray studies[13 14] with two 2 mm cores where PD-L1 expression is minimally represented in tissue microarray cores because of the low expression level on tumour cells and heterogeneous distribution enriched at the invasive front[15] and (C) inadequate numbers of Epstein-Barr virus (EBV)-positive (EBV$^+$) or microsatellite instability-high (MSI-H) GC subtypes, warranting further comprehensive studies. In the present study, we investigated the clinicopathological characteristics and prognostic effects of PD-L1/TIL TME subtypes in a large GC cohort with a full section of tissue in gastric adenocarcinoma and correlated them with MSI-H GC sequencing results.

MATERIAL AND METHODS

Patient selection

Patients who underwent surgery for primary GC tissues from September 2004 to May 2012 at the Samsung Medical Center were used for this study. Among them, 43 EBV$^+$ cases, 79 MSI-H cases and 125 EBV$^-$/microsatellite stable (MSS) GC cases were selected from previous studies.[16–19] All 247 patients underwent curative radical gastrectomy with D2 lymph node dissection, with or without adjuvant chemoradiation therapy (INT-0116 regimen).[20] The mean follow-up period was 48.4±20.1 months. Four patients developed cancer in other organ (lung, skin, pancreas and colon) during the follow-up period. Tumour stage was defined according to TNM classification described in the seventh edition of the American Joint Committee on Cancer (AJCC) cancer staging manual.[21] All patients provided informed consent according to our institutional guidelines.

Subclassification of GCs based on microsatellite instability and EBV

For microsatellite analysis, we performed multiplex PCR with five quasimonomorphic mononucleotide repeat markers as described previously.[22] Samples with no allelic size variations in less than two of the microsatellites were classified as MSS. Tumours with allelic size variations in two or more of the microsatellite markers were considered as MSI-H.

For EBV-encoded RNA (EBER) in situ hybridisation, formalin-fixed paraffin-embedded tissue blocks were used for EBER in situ hybridisation. Three-micrometer thick sections were cut from each block and mounted on Superfrost-plus slides (Thermo Scientific, Waltham, Massachusetts, USA). The entire procedure was performed on a fully automatic system (BOND-MAX) with an EBV-encoded RNA probe from Leica (Newcastle, UK) following manufacturer's instructions. Only cases with a strong signal within all tumour cell nuclei were considered to be positive as previously described.[16]

Based on results of MSI test and EBV status, 247 GC was classified as 79 MSI-H, 43 EBV$^+$ and 125 EBV$^-$/MSS subtypes.

Immunohistochemistry (IHC) and interpretation of PD-L1 and CD8

We performed IHC on whole sections of all 247 GC samples. Staining for PD-L1 in formalin-fixed, paraffin-embedded (FFPE) tissue sections was conducted using an Food and Drug Administration (FDA)-approved rabbit antihuman PD-L1 (clone SP142; Ventana, Tucson, Arizona, USA). Staining for CD8 in FFPE tissue sections was conducted using a CONFIRM-anti-CD8 (SP57) rabbit monoclonal primary antibody without dilution with Ventana BenchMark XT via the OptiView DAB IHC Detection Kit (catalogue number 760–700; Ventana). The IHC slides were interpreted manually via microscopy by two pathologists (JC and K-MK).

The percentages of positively stained on tumour cells (PD-L1^{TC}) and intratumoural and peritumoural immune cells (PD-L1^{IC}) stained positive for PD-L1 were analysed independently. A PD-L1^{TC} was considered positive for PD-L1 if there was histological evidence of membranous and/or cytoplasmic staining. The percentages of PD-L1-positive tumour cells were quantified as 1%, 2%, 3%–5%, 6%–10% and then in 10% increments up to 100%. Based on our preliminary statistical analyses and a previous publication on GC,[23] more than 1% was defined as the criteria for PD-L1^{TC+}. For intratumoural and peritumoural immune cells, a score of 0, 1+, 2+ or 3+ was given when <1%, ≥1% but <5%, ≥5% but <10% or ≥10% of cells per area were PD-L1-positive, respectively, as described previously.[24] The combined positive score (CPS) was calculated by summing the percentage values of PD-L1^{TC+} and PD-L1^{IC+}.[25]

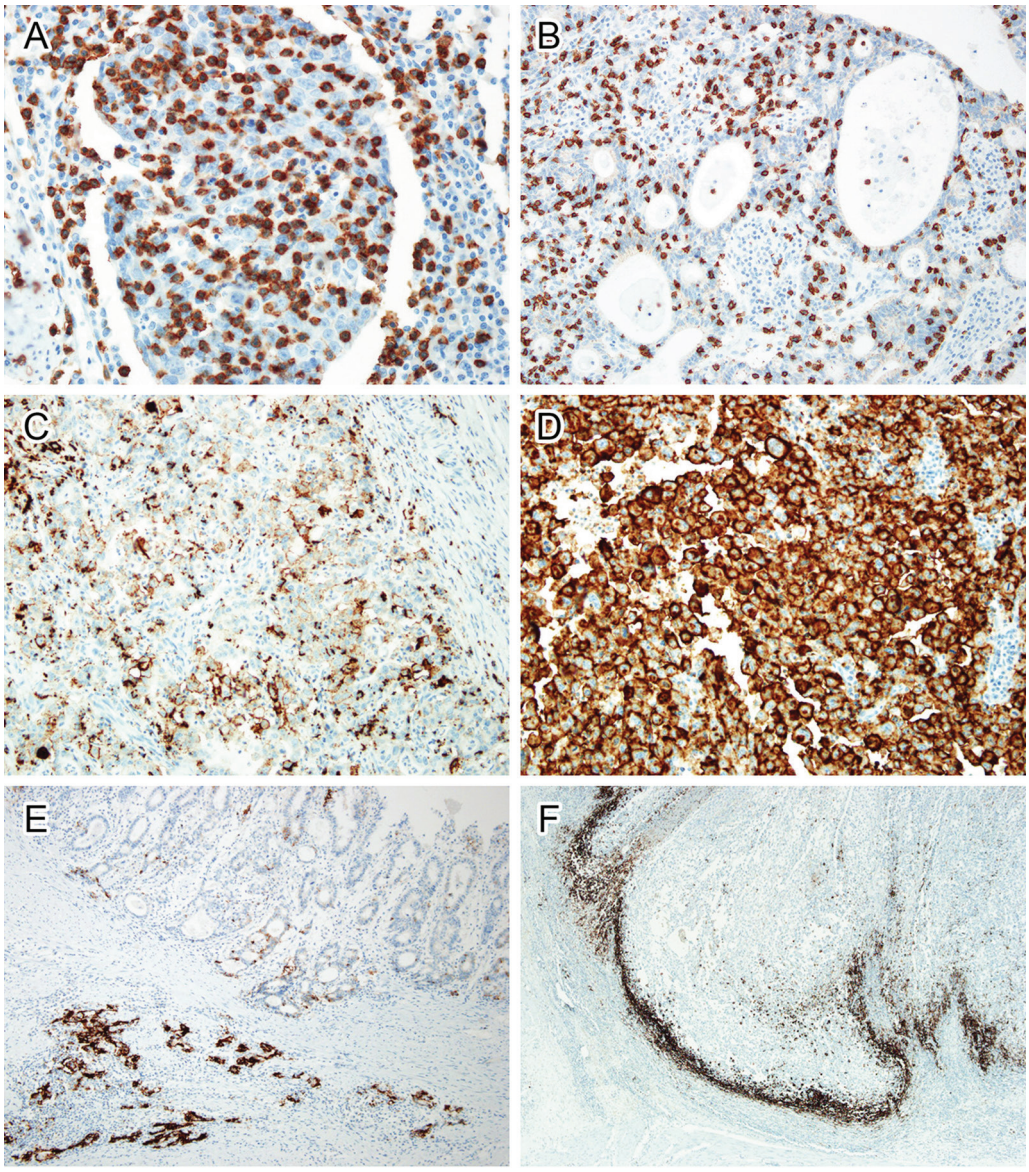

Figure 1 Immunohistochemistry of CD8 (A and B) and PD-L1 (C–F). Intratumoural CD8-positive T cells were more (A) or less (B) numerous than cancer cells. In PD-L1 staining, tumour cells were weakly stained in (C) or strongly stained (D) in the cellular membrane. Both intensities were considered positive staining. In some cases, tumour cells demonstrated marked heterogeneity in PD-L1 expression (E). Well-differentiated tumour cells on the surface were PD-L1 negative, while infiltrating cell nests in the submucosal layer were strongly positive for PD-L1. PD-L1 was predominantly stained in immune cells at the invasive front (F). PD-L1, programmed death-ligand 1.

The distribution of $CD8^+$ T cells was also analysed independently by two pathologists (JC and K-MK). When $CD8^+$ T cells were minimally scattered exclusively in the intratumoural area, the cases were considered as $CD8^{null}$. Cases with innumerable (many) $CD8^+$ T cells within and around cancer cells were interpreted as $CD8^{marked}$ (figure 1A). Cases with moderate $CD8^+$ T cells around cancer cells where the number of $CD8^+$ lymphocytes were smaller than that of cancer cells were interpreted as $CD8^{moderate}$ (figure 1B). Both $CD8^{moderate}$ and $CD8^{marked}$ were considered TIL positive (TIL^+). To reduce interobserver variation, all cases were reviewed by the two pathologists, and in cases of disagreement, the final interpretation was determined by consensus using a multihead microscope.

Deep targeted sequencing of DNA

Genomic DNA (250 ng) from FFPE tissue was sheared in a Covaris S220 ultrasonicator (Covaris, Woburn, Massachusetts, USA) and used for library construction with SureSelect XT reagent kit, HSQ (Agilent Technologies, Santa Clara, California, USA) based on the manufacturer's protocol. This panel is designed to enrich exons of 381 cancer-related genes. After enriched exome libraries were multiplexed, the libraries were sequenced on a HiSeq 2500 sequencing

platform (Illumina, San Diego, California, USA). Sequence reads were mapped to the human genome (hg19) using the Burrows-Wheeler Aligner and duplicate read removal by Picard and SAMtools. Local alignment was optimised using the Genome Analysis Toolkit as previously described.[23 26]

Statistical analysis

We analysed the clinicopathological characteristics such as age, gender, pTNM stage (AJCC seventh edition), disease-free survival (DFS) and overall survival (OS) of patients. We used the SPSS V.18.0 statistical software program for statistical analyses. We compared PD-L1 and CD8 IHC expression and clinicopathological variables using the Pearson's χ^2 test. These test results were further compared using linear-by-linear association. The mean values of the PD-L1 ratio and CD8 ratio were compared by Kruskal-Wallis test. We used the Kaplan-Meier method to estimate DFS and OS. To evaluate the association between clinicopathological variables and survival, the Cox proportional hazard model was used. P values less than 0.05 were considered statistically significant.

RESULTS

PD-L1 and CD8 IHC in gastric carcinomas

The clinicopathological characteristics of the 247 patients with GC are summarised in online supplementary table 1. The PD-L1 IHC on tumour cells (PD-L1^{TC}) varied from weak focal to strong diffuse staining (figure 1C,D). In 7.3% of cases (18 cases), we observed remarkable heterogeneity of PD-L1^{TC} expression (figure 1E). PD-L1 IHC on immune cells (PD-L1^{IC}) was mostly concentrated along the invasive front of the tumour (figure 1F).

The pie charts of PD-L1^{TC}, PD-L1^{IC} and CD8 IHC are depicted in figure 2. PD-L1^{TC+} was frequently observed in 88.4% of EBV^{+} GC followed by MSI-H GC and EBV^{-}/MSS GC. PD-L1^{IC+} with ≥1% of tumour volume (PD-L1$^{IC\ 1+}$) was most frequently observed in EBV^{+} GC (93.0%), while PD-L1^{IC+} with ≥10% (PD-L1$^{IC\ 3+}$) was most frequent in MSI-H GC (63.3%).

CPS with ≥1 (PD-L1$^{CPS\geq1}$) was most frequent in EBV^{+} GC (90.7%), followed by MSI-H GC (84.8%) and EBV^{-}/MSS (31.2%), while PD-L1$^{CPS\geq10}$ was highest in MSI-H (62.0%), followed by EBV^{+} (55.8%) and EBV^{-}/MSS (7.2%) GC. CD8^{+} (moderate and marked infiltrates of CD8-positive cells) was most marked in EBV^{+} GC (95.3%) followed by MSI-H GC (81%) and EBV^{-}/MSS GC (40.8%). EBV^{-}/MSS GC showed the lowest positive rate in both PD-L1 and CD8^{+}.

Kaplan-Meier survival analyses of PD-L1 and CD8 IHC affecting each subtype of GC are shown in online supplementary figure. In survival analysis of all patients, PD-L1^{TC+} (DFS: P=0.001; OS: P<0.001), PD-L1$^{IC\ 3+}$ (DFS: P=0.010; OS: P=0.005) and CD8^{marked} (DFS: P=0.003; OS: P<0.001) were significant prognostic factors in both DFS and OS of patients.

PD-L1 and CD8 IHC in MSI-H GC and correlation with mutation loads

In the MSI-H subtype of GC (n=79), PD-L1^{TC+} were observed in 56 (70.9%) cases and PD-L1^{IC3+} was found in 50 (63.3%) cases. GC with PD-L1$^{CPS\geq1}$ was observed in 67 (84.8%) cases. In all MSI-H GC cases, we performed deep targeted sequencing and obtained good quality sequencing results in 66 cases. The mean number of somatic (cancer only) single-nucleotide variants (SNVs) was 61.71 (range: 9–269), and the mean number of frameshift mutations was 18.88 (range: 1–42). A more detailed description of the sequencing quality, SNV and frameshift mutations found in 66 MSI-H GC are described in online supplementary tables 2–4. Most frameshift mutations were observed in *ARID1A*, *RNF43*, *NF1*, *MSH6*, *BRD3*, *NCOA3*, *BCORL1*, *TNKS2* and *NPM1*. The sum of SNVs and frameshift mutations was not significantly correlated with age, sex, location of tumour, histological type by Lauren, host inflammatory responses, PD-L1^{TC} or CD8. However, the number of frameshift mutation was significantly higher in cases with PD-L1^{TC+} compared with PD-L1^{TC-} (P=0.045) and PD-L1$^{IC\ 1+}$ than PD-L1^{IC-} (P=0005). In the CPS analyses, the higher number of frameshift mutation was significantly correlated with higher CPS when the cut-off value was set to 2 (P=0.009), 5 (P=0.006) or 10 (P=0.037) points (table 1). However, the number of frameshift mutation or SNV was not significantly associated with survival.

TME (PD-L1/TIL) subtypes

Of all 247 patients with GC, we classified the TME subtypes based on the PD-L1^{TC+} and degrees of CD8 infiltration (TIL). It consists of type I (PD-L1^{TC+}/TIL^{+}) in 107 (43.3%) cases, type II (PD-L1^{TC-}/TIL^{-}) in 66 (26.7%) cases, type III (PD-L1^{TC+}/TIL^{-}) in 25 (10.1%) cases and type IV (PD-L1^{TC-}/TIL^{+}) in 49 (19.8%) cases. The clinicopathological characteristics of the four TME types are summarised in table 2. In survival analyses, the prognosis of TME type I exhibited the best prognosis in both DFS (P=0.005) and OS (P<0.001), followed by type III and IV, with the worst prognosis exhibited by type II (figure 3). In multivariate analysis, TME type I was an independent favourable prognostic factor in OS (HR: 2.325; 95% CI 1.201 to 4.502; P=0.038; online supplementary table 5). PD-L1 and CD8, which were significant prognostic markers in the univariate survival analyses, were unable to predict prognosis of GC independently.

DISCUSSION

The TCGA and ACRG-SMC proposed that GC should be categorised into four molecular subtypes.[19 27] Interestingly, nearly 50% of EBV^{+} and 60% of MSI-H GC subgroups showed high levels of PD-L1 expression, highlighting the molecularly defined patient population most likely to derive benefit from immune checkpoint blockade.[28–30] The frequency of PD-L1 (a putative response biomarker) expression approached 40% in GC.

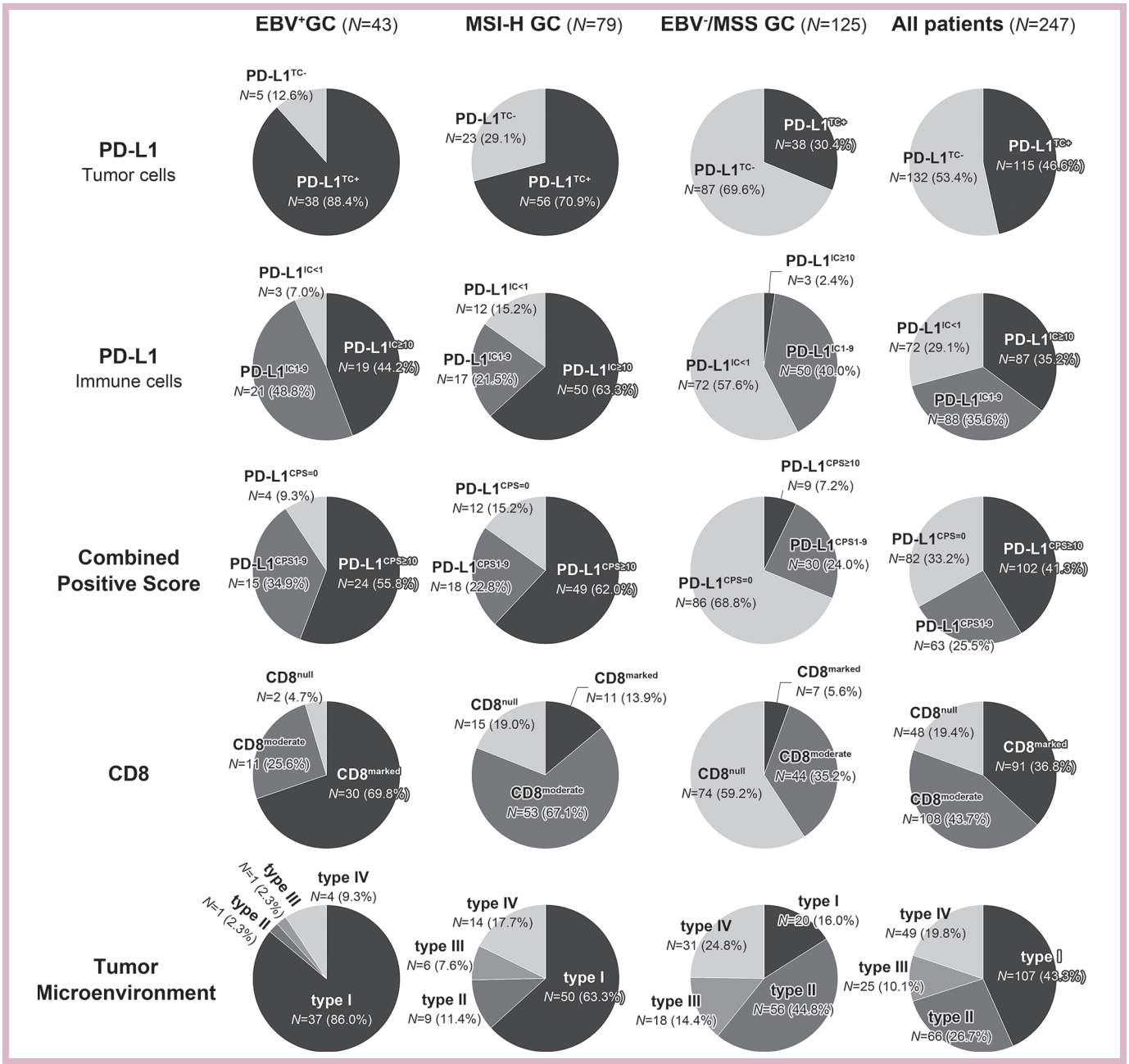

Figure 2 Pie charts of PD-L1 and CD8 immunohistochemistry. The proportions of PD-L1^{TC+}, PD-L1$^{CPS\geq1}$, CD8^{marked} and TME type I were most frequently observed in EBV^{+} GC, while the proportion of PD-L1$^{IC\geq10}$ was the highest in MSI GC. GC, gastric cancer; PD-L1, programmed death-ligand 1; TME, tumour microenvironments.

However, not all EBV^{+} or MSI-H GC overexpress PD-L1, and PD-L1 can be overexpressed in tumours other than EBV^{+} or MSI-H GC. Therefore, this warrants further TME classifications in association with the treatment strategies for immunotherapy. In this study, we aimed to identify a TME classification of GC to better understand tumour–immune interactions and help in patient selection for future immunotherapy. We measured the expression of PD-L1 and CD8^{+} T cell density in three distinct subtypes of GC (EBV^{+}/MSI-H/EBV^{-} MSS) in relation to host anti-tumour immunity. We also compared the mutation loads with PD-L1 expression and survival in MSI-H GC patients.

In this study, we performed PD-L1 IHC with the FDA-approved SP142 antibody in a whole section of 247 surgically resected GC and included a significant number of EBV^{+} (n=43) and MSI-H (n=79) GC to evaluate the PD-L1 expression and intratumoural T cell density as a surrogate marker of TILs. As expected, PD-L1^{TC+}, PD-L1^{IC+}, PD-L1$^{CPS\geq1}$ and CD8^{+} were more frequent in EBV^{+} and MSI-H GC compared with in EBV^{-}/MSS GC. PD-L1 expression in immune cells was more prominent in the invasive margin of tumours, as reported previously.[29 30] PD-L1 positivity in our study was higher than that in previous studies.[13 14 23 31–34] This difference was likely caused by the

Table 1 Kruskal-Wallis tests of the correlation between the number of mutations and immune-related markers in microsatellite instability-high gastric cancer (n=66)

	Number of cases (%)	Number of frameshift mutation		Number of SNV		Sum of frameshift and SNV	
		Mean rank	P values	Mean rank	P values	Mean rank	P values
Histology by HIR							
CA	16 (24.2)	32.88	0.881	29.47	0.334	29.44	0.331
CLR	50 (75.8)	33.7		34.79		34.80	
PD-L1^{TC}							
Positive	29 (43.9)	38.84	0.045	37.55	0.129	38.45	0.064
Negative	37 (56.1)	29.31		30.32		29.62	
PD-L1^{IC}							
≥1%	60 (90.9)	35.58	0.005	34.80	0.082	35.01	0.043
<1%	6 (9.1)	12.75		20.50		18.42	
≥10%	49 (74.2)	35.96	0.077	35.26	0.207	35.49	0.153
<10%	17 (25.8)	26.41		28.44		27.76	
CPS							
≥2	59 (89.4)	35.62	0.009	34.71	0.136	34.97	0.070
<2	7 (10.6)	15.64		23.29		21.07	
≥5	56 (84.8)	36.25	0.006	34.11	0.543	34.62	0.264
<5	10 (15.2)	18.10		30.10		27.25	
≥10	50 (75.8)	36.28	0.037	35.11	0.228	35.45	0.145
<10	16 (24.2)	24.81		28.47		27.41	
CD8							
Null	14 (21.2)	30.21	0.667	27.11	0.373	27.43	0.410
Moderate	43 (65.2)	33.73		35.23		35.07	
Marked	9 (13.6)	37.50		35.17		35.44	

CA, conventional adenocarcinoma; CLR, carcinoma with Crohn-like reaction; CPS, combined positive score; HIR, host immune response; PD-L1, programmed death-ligand 1; SNV, single-nucleotide variant.

high numbers of EBV$^+$/MSI-H GC compared with those in previous studies, and we used whole tissue blocks for this study rather than tissue microarray. We found that PD-L1^{TC+}, PD-L1^{IC+}, PD-L1$^{CPS\geq1}$ and CD8$^+$ were significantly favourable prognostic factors in all 247 GC patients but lost their significance in GC subtype analyses.

Based on melanoma studies, we divided the GC TME classifications with PD-L1 IHC and intratumoural CD8 density. The proportions of various human tumours that fit into each of these types, as defined by PD-L1/TIL status, likely depends on the genetic aberrations and oncogene drivers of the cancer as well as the tissue in which they arise.[9] In advanced melanoma, ~38% of patients presented with a type I TME and were predicted to benefit from the single agent anti-PD-1/L1 blockade.[9] In this study, we found that ~40% of patients with GC and ~70% of MSI-H and EBV$^+$ GC patients were in this group and that they may respond to checkpoint blockade. Unexpectedly, we found that ~15% of EBV$^-$/MSS GC patients were also included in this type I group. As expected, we found that type I showed the best survival in both DFS and OS and that the significance remained even in multivariate analyses. PD-L1 positivity in the TME type I may be adaptive PD-L1 expression in tumour cells caused by external stimuli such as the cytotoxic effect of CD8$^+$ T cells.[9] In our study, the ratio of PD-L1^{TC+} was higher in the CD8$^+$ group (68.6%) than in the CD8$^-$ group (27.5%).

In melanoma, large numbers of melanoma patients (~41%) present type II TME and are predicted to have a very poor prognosis based on their lack of a detectable immune reaction. In our cohort, ~30% of patients were within this type and showed the worst survival. Only 1% of melanoma patients displayed type III TME and ~10% of the GC was within this type; this high incidence is similar to that of other cancers such as non-small cell lung carcinoma.[35] This type occurs when PD-L1 is expressed constitutively on cancer cells through oncogenic signalling. Accordingly, this type was very rare in EBV$^+$ or MSI-H GC patients but was common in EBV$^-$/MSS GC. In this group, radiotherapy to induce immunogenic cell death to liberate neoantigens has been used to induce T cell responses in combination with anti-PD-1.[36] Type IV TME constitutes ~20% of melanoma patients, and we observed ~20% of GC are in this type. Therapeutic

Table 2 Correlation between tumour microenvironment types and clinicopathological features of patients with gastric cancer

	Tumour microenvironment (by manual interpretation)				
	Type I (n=107)	Type II (n=66)	Type III (n=25)	Type IV (n=49)	
	No.(%)	No.(%)	No.(%)	No.(%)	P values
Age					
<60	46 (43.0)	38 (57.6)	13 (52.0)	26 (53.1)	0.280*
≥60	61 (57.0)	28 (42.4)	12 (48.0)	23 (46.9)	
Sex					
Male	86 (80.4)	37 (56.1)	19 (76.0)	25 (51.0)	<0.001*
Female	21 (19.6)	29 (43.9)	6 (24.0)	24 (49.0)	
Location					
Antrum	47 (43.9)	26 (39.4)	13 (52.0)	17 (34.7)	0.486*
Others	60 (56.1)	40 (60.6)	12 (48.0)	21 (65.3)	
Subtype					
EBV(+)	37 (34.6)	1 (1.5)	1 (4.0)	4 (8.2)	<0.001*
MSI-H	50 (46.7)	9 (13.6)	6 (24.0)	14 (28.6)	
EBV(-)/MSS	20 (18.7)	56 (84.8)	18 (72.0)	31 (63.3)	
Histological type by Lauren					
Intestinal	48 (44.9)	22 (33.3)	13 (52.0)	20 (40.8)	0.001*
Mixed	11 (10.3)	5 (7.6)	4 (16.0)	2 (4.1)	
Diffuse	37 (34.6)	39 (59.1)	8 (32.0)	27 (55.1)	
Indeterminate	11 (10.3)	0 (0.0)	0 (0.0)	0 (0.0)	
Histological type by host inflammatory response					
CA	33 (30.8)	47 (71.2)	19 (76.0)	27 (55.1)	<0.001*
CLR	50 (46.7)	19 (28.8)	6 (24.0)	19 (38.8)	
LELC	24 (22.4)	0 (0.0)	0 (0.0)	3 (6.1)	
pT					
1	10(9.3)	5(7.6)	1(4.0)	0 (0.0)	0.126†
2	56(52.3)	21(31.8)	12(48.0)	22 (44.9)	
3	25(23.4)	22(33.3)	9(36.0)	21 (42.9)	
4	16(15.0)	18(27.3)	3(12.0)	6 (12.2)	
pN					
0	39 (36.4)	12 (18.2)	6 (24.0)	12 (24.5)	0.106†
1	32 (29.9)	28 (42.4)	7 (28.0)	18 (36.7)	
2	28 (26.2)	14 (21.2)	4 (16.0)	14 (28.6)	
3	8 (7.5)	12 (18.2)	8 (32.0)	5 (10.2)	
TNM stage					
I	31(29.0)	9(13.6)	3(12.0)	8(16.3)	0.001†
II	41(38.3)	20(30.3)	9(36.0)	14(28.6)	
III	32(29.9)	30(45.5)	11(44.0)	19(38.8)	
IV	3(2.8)	7(10.6)	2(8.0)	8(16.3)	
Distant metastasis					
Absent	103(96.3)	56 (84.8)	20 (80.0)	39 (79.6)	0.006*
Present	4(3.7)	10 (15.2)	5 (20.0)	10 (20.4)	

*Pearson's χ^2 test.
†Linear-by-linear association.
CA, conventional adenocarcinoma; CLR, carcinoma with Crohn-like reaction; EBV, Epstein-Barr virus; LELC, lymphoepithelioma-like carcinoma; MSI-H, microsatellite instability-high; MSS, microsatellite stable; pT, pathologic T; pN, pathologic N, TNM, tumor/node/metastasis.

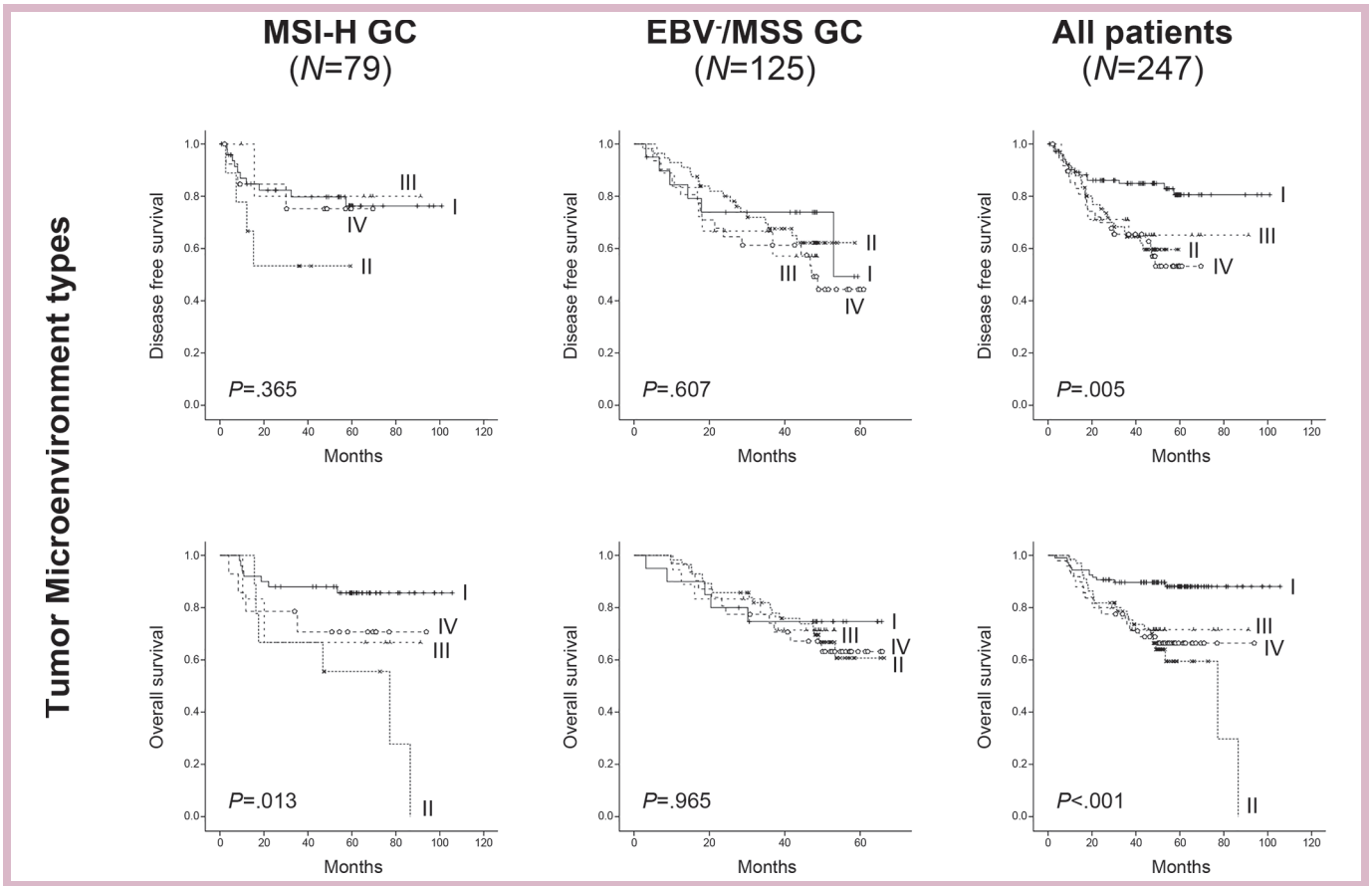

Figure 3 Kaplan-Meier survival curves for tumour microenvironment types in each GC subgroup. In EBV$^+$ GC (n=43), all cases were censored and P values were not calculated. GC, gastric cancer; MSI-H, microsatellite instability-high.

approaches for type IV TME are still limited, but many approaches will likely enter the clinic in the near future.[9] Notably, ~25% of EBV$^+$ and MSI-H GC harbour type IV TME, warranting more investigation of this type. Nevertheless, our observations suggest that TME plays a key role in the progression of GC.

In the present study, we also compared the mutation loads with PD-L1 expression and survival in 66 MSI-H GC and found that the number of frameshift mutations was significantly higher in PD-L1-positive cases than in PD-L1-negative cases. Mutations have the capacity to encode neoantigens that are specific to a tumour and relative to normal somatic cells.[37] The association of the MSI-H phenotype with the presence of TILs is explained by the accumulation of frameshift mutations and synthesis of neoantigens that trigger the host immune system.[38] In this study, although we tested mutation loads in MSI-H GC only, we first found that the number of frameshift mutation was significantly higher in PD-L1-positive cases and correlated with PD-L1 CPS. Our observations are consistent with a previous hypothesis in MSI-H colon cancer that T cell infiltrate was interlaced with an abundant PD-L1 positive myeloid cell population, which presumably inhibited the T cell response and overlapped with melanoma where neoantigens cause PD-L1 expression in tumour cells.[39 40]

In conclusion, GC can be classified into four TME groups according to PD-L1 expression and TIL. TME type I, which is expected to be suitable for anti-PD-1/PD-L1 immunotherapy, was more frequent in EBV$^+$ and MSI-H GC, but also found in ~15% of EBV$^-$/MSS GC and was associated with favourable prognosis. Frameshift mutations correlating well with PD-L1 expression suggest that frameshift mutation-derived tumour-specific neoantigens also exist in MSI-H GC.

Contributors All authors listed on this manuscript declare that they were equally involved in the data acquisition and interpretation of data and manuscript writing and review for this submitted work.

Funding This research was supported by a grant (NRF-2017R1A2B4012436, NRF-2017R1D1A1B03032449 and 2017R1E1A1A01075005) from the National Research Foundation of Korea (NRF).

Competing interests None declared.

Patient consent Obtained.

Ethics approval Samsung Medical Center.

Provenance and peer review Not commissioned; externally peer reviewed.

REFERENCES

1. Ang YL, Yong WP, Tan P. Translating gastric cancer genomics into targeted therapies. *Crit Rev Oncol Hematol* 2016;100:141–6.
2. Jemal A, Bray F, Center MM, *et al*. Global cancer statistics. *CA Cancer J Clin* 2011;61:69–90.
3. Tang H, Qiao J, Fu YX, Yx F. Immunotherapy and tumor microenvironment. *Cancer Lett* 2016;370:85–90.
4. Ni L, Dong C. New checkpoints in cancer immunotherapy. *Immunol Rev* 2017;276:52–65.
5. Park C, Cho J, Lee J, *et al*. Host immune response index in gastric cancer identified by comprehensive analyses of tumor immunity. *Oncoimmunology* 2017;6:e1356150.
6. Taube JM, Anders RA, Young GD, *et al*. Colocalization of inflammatory response with B7-h1 expression in human melanocytic lesions supports an adaptive resistance mechanism of immune escape. *Sci Transl Med* 2012;4:127ra37.
7. Hino R, Kabashima K, Kato Y, *et al*. Tumor cell expression of programmed cell death-1 ligand 1 is a prognostic factor for malignant melanoma. *Cancer* 2010;116:1757–66.
8. Dong H, Strome SE, Salomao DR, *et al*. Tumor-associated B7-H1 promotes T-cell apoptosis: a potential mechanism of immune evasion. *Nat Med* 2002;8:793–800.
9. Teng MW, Ngiow SF, Ribas A, *et al*. Classifying Cancers Based on T-cell Infiltration and PD-L1. *Cancer Res* 2015;75:2139–45.
10. Lee JK KM. Biomarkers for gastric cancer: molecular classification revisited. *Precision and Future medicine* 2017;1:59–68.
11. Fridman WH, Pagès F, Sautès-Fridman C, *et al*. The immune contexture in human tumours: impact on clinical outcome. *Nat Rev Cancer* 2012;12:298–306.
12. Thompson ED, Zahurak M, Murphy A, *et al*. Patterns of PD-L1 expression and CD8 T cell infiltration in gastric adenocarcinomas and associated immune stroma. *Gut* 2017;66:794–801.
13. Kawazoe A, Kuwata T, Kuboki Y, *et al*. Clinicopathological features of programmed death ligand 1 expression with tumor-infiltrating lymphocyte, mismatch repair, and Epstein-Barr virus status in a large cohort of gastric cancer patients. *Gastric Cancer* 2017;20:407–15.
14. Koh J, Ock CY, Kim JW, *et al*. Clinicopathologic implications of immune classification by PD-L1 expression and CD8-positive tumor-infiltrating lymphocytes in stage II and III gastric cancer patients. *Oncotarget* 2017;8:26356–67.
15. .Botti G, Scognamiglio G, Cantile M. PD-L1 Immunohistochemical Detection in Tumor Cells and Tumor Microenvironment: Main Considerations on the Use of Tissue Micro Arrays. *Int J Mol Sci* 2016;17:1046.
16. Song HJ, Srivastava A, Lee J, *et al*. Host inflammatory response predicts survival of patients with Epstein-Barr virus-associated gastric carcinoma. *Gastroenterology* 2010;139:84–92.
17. Lee J, Lim DH, Kim S, *et al*. Phase III trial comparing capecitabine plus cisplatin versus capecitabine plus cisplatin with concurrent capecitabine radiotherapy in completely resected gastric cancer with D2 lymph node dissection: the ARTIST trial. *J Clin Oncol* 2012;30:268–73.
18. Lee J, Sohn I, Do IG, *et al*. Nanostring-based multigene assay to predict recurrence for gastric cancer patients after surgery. *PLoS One* 2014;9:e90133.
19. Cristescu R, Lee J, Nebozhyn M, *et al*. Molecular analysis of gastric cancer identifies subtypes associated with distinct clinical outcomes. *Nat Med* 2015;21:449–56.
20. Macdonald JS, Smalley SR, Benedetti J, *et al*. Chemoradiotherapy after surgery compared with surgery alone for adenocarcinoma of the stomach or gastroesophageal junction. *N Engl J Med* 2001;345:725–30.
21. American Joint Commitee on Cancer. *AJCC Cancer Staging Manual*. 7 edn. Verlag New York: Springer, 2010.
22. Min BH, Tae CH, Ahn SM, *et al*. Epstein-Barr virus infection serves as an independent predictor of survival in patients with lymphoepithelioma-like gastric carcinoma. *Gastric Cancer* 2016;19:852–9.
23. Muro K, Chung HC, Shankaran V, *et al*. Pembrolizumab for patients with PD-L1-positive advanced gastric cancer (KEYNOTE-012): a multicentre, open-label, phase 1b trial. *Lancet Oncol* 2016;17:717–26.
24. Herbst RS, Soria JC, Kowanetz M, *et al*. Predictive correlates of response to the anti-PD-L1 antibody MPDL3280A in cancer patients. *Nature* 2014;515:563–7.
25. Kulangara K, Hanks DA, Waldroup S, *et al*. Development of the combined positive score (CPS) for the evaluation of PD-L1 in solid tumors with the immunohistochemistry assay PD-L1 IHC 22C3 pharmDx. *J Clin Oncol* 2017;35:e14589.
26. Lee C, Bae JS, Ryu GH, *et al*. A Method to Evaluate the Quality of Clinical Gene-Panel Sequencing Data for Single-Nucleotide Variant Detection. *J Mol Diagn* 2017;19:651–8.
27. Cancer Genome Atlas Research Network. Comprehensive molecular characterization of gastric adenocarcinoma. *Nature* 2014;513:202–9.
28. Raufi AG, Klempner SJ. Immunotherapy for advanced gastric and esophageal cancer: preclinical rationale and ongoing clinical investigations. *J Gastrointest Oncol* 2015;6:561–9.
29. Lee KS, Kwak Y, Ahn S, *et al*. Prognostic implication of CD274 (PD-L1) protein expression in tumor-infiltrating immune cells for microsatellite unstable and stable colorectal cancer. *Cancer Immunol Immunother* 2017;66:927–39.
30. Derks S, Liao X, Chiaravalli AM, *et al*. Abundant PD-L1 expression in Epstein-Barr Virus-infected gastric cancers. *Oncotarget* 2016;7:32925–32.
31. Geng Y, Wang H, Lu C, *et al*. Expression of costimulatory molecules B7-H1, B7-H4 and Foxp3+ Tregs in gastric cancer and its clinical significance. *Int J Clin Oncol* 2015;20:273–81.
32. Schlößer HA, Drebber U, Kloth M, *et al*. Immune checkpoints programmed death 1 ligand 1 and cytotoxic T lymphocyte associated molecule 4 in gastric adenocarcinoma. *Oncoimmunology* 2016;5:e1100789.
33. Kim JW, Nam KH, Ahn SH, *et al*. Prognostic implications of immunosuppressive protein expression in tumors as well as immune cell infiltration within the tumor microenvironment in gastric cancer. *Gastric Cancer* 2016;19:42–52.
34. Wu Y, Cao D, Qu L, *et al*. PD-1 and PD-L1 co-expression predicts favorable prognosis in gastric cancer. *Oncotarget* 2017;8.
35. D'Incecco A, Andreozzi M, Ludovini V, *et al*. PD-1 and PD-L1 expression in molecularly selected non-small-cell lung cancer patients. *Br J Cancer* 2015;112:95–102.
36. Kalbasi A, June CH, Haas N, *et al*. Radiation and immunotherapy: a synergistic combination. *J Clin Invest* 2013;123:2756–63.
37. Topalian SL, Taube JM, Anders RA, *et al*. Mechanism-driven biomarkers to guide immune checkpoint blockade in cancer therapy. *Nat Rev Cancer* 2016;16:275–87.
38. Woerner SM, Gebert J, Yuan YP, *et al*. Systematic identification of genes with coding microsatellites mutated in DNA mismatch repair-deficient cancer cells. *Int J Cancer* 2001;93:12–19.
39. Xiao Y, Freeman GJ. The microsatellite instable subset of colorectal cancer is a particularly good candidate for checkpoint blockade immunotherapy. *Cancer Discov* 2015;5:16–18.
40. Llosa NJ, Cruise M, Tam A, *et al*. The vigorous immune microenvironment of microsatellite instable colon cancer is balanced by multiple counter-inhibitory checkpoints. *Cancer Discov* 2015;5:43–51.